Membrane and Water Treatment, *Vol. 16, No. 2 (2025) 77-86*
https://doi.org/10.12989/mwt.2025.16.2.077

Evaluation of CO_2 absorbent-based draw solution as draw solution for forward osmosis treatment of domestic wastewater

Sehyuk Ahn[1], Jieun Kim[2], Jeongkyun Yu[2], Hyunsup Jang[3], Sangyoup Lee[4], Ihn-Sup Han[*1] and Youngjin Kim[**2]

[1]*School of Environmental Engineering, University of Seoul, Siripdae-gil 13, Dongdaemun-gu, Seoul, 02504, Republic of Korea*
[2]*Department of Environmental Engineering, College of Science and Technology, Korea University, 2511, Sejong-ro, Sejong, 30019, Republic of Korea*
[3]*Environmental Forensic Lab, Sungkyunkwan University, 2066, Seobu-ro, Jangan-gu, Suwon-si, Republic of Korea*
[4]*Institute of Conversions Science, Korea University, 145, Anam-ro, Sungbuk-gu, Seoul 02841, Republic of Korea*

(Received January 1, 2025, Revised February 17, 2025, Accepted February 24, 2025)

Abstract. This study investigates the feasibility of using sodium carbonate (Na_2CO_3) and sodium bicarbonate ($NaHCO_3$), by-products of carbon dioxide (CO_2) capture processes, as draw solutions (DSs) in forward osmosis (FO) systems. The primary objectives were to evaluate the basic performance of these DSs, analyze membrane fouling behaviors, and assess economic feasibility. The FO process demonstrated superior water flux performance with Na_2CO_3, attributed to its high osmotic pressure, followed by $NaHCO_3$ and sodium chloride (NaCl). Fouling analysis revealed that Na_2CO_3 mitigates fouling due to its alkaline nature, which inhibits biofouling and scaling. Economic evaluations confirmed Na_2CO_3 as the most cost-effective DS, offering significant cost savings over $NaHCO_3$ and NaCl at all recovery levels. These findings highlight the potential of Na_2CO_3 as a sustainable and efficient DS for wastewater treatment and other FO applications, emphasizing its compatibility with CO_2 capture technologies.

Keywords: adsorbent; carbon capture; domestic wastewater; draw solution; forward osmosis

1. Introduction

Carbon dioxide (CO_2), a prominent greenhouse gas, primarily originates from the combustion of conventional fuels for energy production. Elevated levels of CO_2 in the atmosphere contribute to global warming, triggering a cascade of environmental issues such as natural disasters, rising sea levels, and disruptions to ecosystems. Addressing this critical global warming challenge, Carbon Capture, Utilization, and Storage (CCUS) technology has emerged as a solution. CCUS technology is designed to capture CO_2 emissions from industrial processes, subsequently repurposing it, and securely storing the remaining CO_2 (Hong 2022). The adoption of CCUS technology holds substantial promise in significantly curbing greenhouse gas emissions and mitigating the effects of climate change.

To employ CCUS technology for capturing CO_2 emissions from various industries or thermal power plants, the utilization of CO_2 absorbents is a common practice (Li *et al*. 2013). CO_2 absorbents work by chemically binding with CO_2, rendering it suitable for safe storage or alternative applications. Frequently utilized CO_2 absorbents encompass amines and carbonates. Amines react with CO_2 to produce carbamate or carbamic acid (Said *et al*. 2020), while carbonates yield stable metal carbides (Salminen and Kobylin 2006). Recent research has also explored solid absorbents like zeolites and metal- organic frameworks for CO_2 capture (Sumida *et al*. 2012, Megías-Sayago *et al*. 2019). The choice of absorbent for CO_2 capture hinges on factors such as the concentration of CO_2 in the exhaust gas, operating temperature, pressure conditions, and the intended use of the captured CO_2 (Tiwari *et al*. 2022).

$$2NaOH + CO_2 \rightarrow Na_2CO_3 + H_2O \quad (1)$$

$$Na_2CO_3 + CO_2 + H_2O \rightarrow 2NaHCO_3 \quad (2)$$

Sodium hydroxide, abbreviated as NaOH, stands out as an exceptionally effective CO_2 absorbent in CCUS technologies (Yincheng *et al*. 2011). As demonstrated in Eq. (1), NaOH readily forms Na_2CO_3 when it reacts with CO_2 (Yoo *et al*. 2013). Notably, NaOH's distinct advantage lies in its remarkably high reactivity with CO_2, enabling swift and efficient CO_2 absorption. Furthermore, NaOH boasts the benefits of wide availability and cost-effectiveness compared to other absorbents. Moreover, Na_2CO_3, a by-product of the NaOH-CO_2 reaction, holds the potential to enhance CCUS utilization across multiple industries (Hocking 2005). Na_2CO_3 plays a key role in the CCUS process, offering affordability, high utilization rates, and strong CO_2 capture capacity (Yoo *et al*. 2013). It can react with CO_2 to form $NaHCO_3$ as a by-product and allows easy separation and recovery of captured CO_2 through a reversible reaction (Toan *et al*. 2019).

The forward osmosis (FO) process is a technique for extracting clean water from contaminated sources, which

[*]Corresponding author, Professor,
E-mail: ishan@uos.ac.kr

[**]Co-corresponding author, Professor,
E-mail: kyuksh@korea.ac.kr

ISSN: 2005-8624 (Print), 2092-7037 (Online)

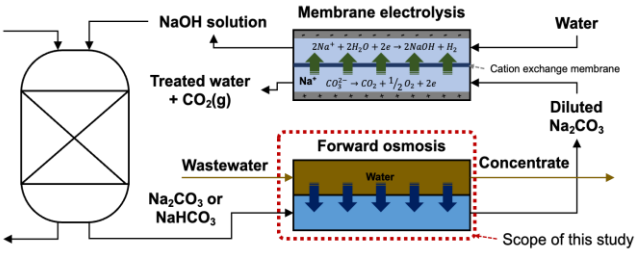

Fig. 1 Schematic diagram of CO_2 capture and wastewater treatment processes

Table 1 Characteristics of FO membranes used in this study

Draw solutions	Water permeability ($L/m^2/h/bar$)	Salt permeability ($L/m^2/h$)	Structural parameter (μm)
NaCl		0.73	
$NaHCO_3$	3.07	0.51	197
Na_2CO_3		1.08	

Table 2 Detailed composition of the synthetic domestic wastewater used in this study (Chekli *et al*. 2017)

Compounds	Concentration
Glucose (mg/L)	275
Peptone (mg/L)	100
Beef extract (mg/L)	100
Urea (mg/L)	10
$NaHCO_3$ (mg/L)	100
KH_2PO_4 (mg/L)	20
NH_4Cl (mg/L)	25
$MgCl_2{\cdot}6H_2O$ (mg/L)	10
$CaCl_2{\cdot}2H_2O$ (mg/L)	5
pH	6.58
Conductivity (mS/cm)	0.226
COD (mg/L)	390

may contain heavy metals and organic pollutants, by employing a semi-permeable membrane in conjunction with a high-concentration inducing solution (Shaffer *et al*. 2015, Benyahia *et al*. 2024). In this method, a low-concentration influent is juxtaposed with a high-concentration inducing solution possessing elevated osmotic pressure. This disparity in osmotic pressure between the semi-permeable membranes prompts the movement of pure water from the low-concentration side to the high-concentration side. Interestingly, the high-concentration Na_2CO_3 or $NaHCO_3$, generated as a by-product during CO_2 capture with NaOH, can serve as a suitable inducing solution for the FO process. These compounds inherently possess the capability to induce high osmotic pressure. In practice, reusing the draw solution (DS) from the FO process and ensuring a sustainable supply of clean water necessitates a method for concentrating the initially diluted DS (Ge *et al*. 2013).

Cation exchange membrane electrolysis technology employs a cation exchange membrane to regulate ion movement and transforms electrical energy into chemical energy using two electrodes (Paidar *et al*. 2016). In this process, the cation exchange membrane permits the passage of cations while hindering the movement of anions. The effectiveness of this procedure is notably influenced by several operational factors, including influent water quality, membrane type, temperature, pressure, and flow rate (Bazarah *et al*. 2022). Notably, the choice of a cation exchange membrane can lead to scaling issues, dependent on the properties of the source water (Sosa-Fernandez *et al*. 2021). Higher operating temperatures are advantageous as they reduce overall power consumption by enhancing ion migration and electrochemical reaction rates (Selamet *et al*. 2013). While flow rate does not substantially affect a process performance, it plays a significant role in bubble formation and temperature control within the system (Majasan *et al*. 2018, Teuku *et al*. 2021). Consequently, this technology is capable of producing NaOH, a CO_2 absorbent, and recovering CO_2 gas from a diluted Na_2CO_3 solution using a FO process.

Fig. 1 illustrates a process that integrates three key components (i.e., a CO_2 capture process, a FO process, and a cation exchange membrane electrolysis process) for wastewater treatment, the generation of high-concentration NaOH and the separation of CO_2 via the cation exchange membrane electrolysis process. There, this integrated process achieves three purposes: CO_2 capture, wastewater treatment, and the recycling of NaOH (i.e., a crucial CO_2 absorbent).

In this system, FO dilution of Na_2CO_3 helps regulate water balance, preventing scaling and reducing wastewater in membrane electrolysis. It also stabilizes ion concentrations, improving membrane longevity and reducing operational issues. While dilution lowers conductivity, proper control can optimize NaOH production and CO_2 evolution while enhancing overall system efficiency.

This study aims to assess the feasibility of employing Na_2CO_3 and $NaHCO_3$, both derived from the CO_2 capture by-products illustrated in Fig. 1, as DSs for the FO process. To achieve this objective, the basic performance of the FO process employing these CO_2 capture by-products, Na_2CO_3 and $NaHCO_3$, was evaluated. Furthermore, the potential for membrane fouling was investigated through long-term operation of the FO process employing synthetic wastewater as the influent. Lastly, an economic evaluation was conducted based on the long-term evaluation.

2. Materials and methods

2.1 FO Membranes

Thin-film composite (TFC) polyamide (PA) FO membrane was obtained from Toray Korea. Membrane samples were extracted from the module and preserved in deionized water at a temperature of 4 ºC. Details about the FO membrane employed in this research are characterized in Table 1.

In this study, a mathematical approach was employed to simultaneously determine these parameters under non-pressurized conditions (Tiraferri *et al*. 2013). Experimental measurements were conducted using a lab-scale FO unit with an effective membrane area of 20.02 cm^2. The operating temperature was maintained at 25 ºC, and the cross-flow velocities of both solutions were set to 25 cm/s.

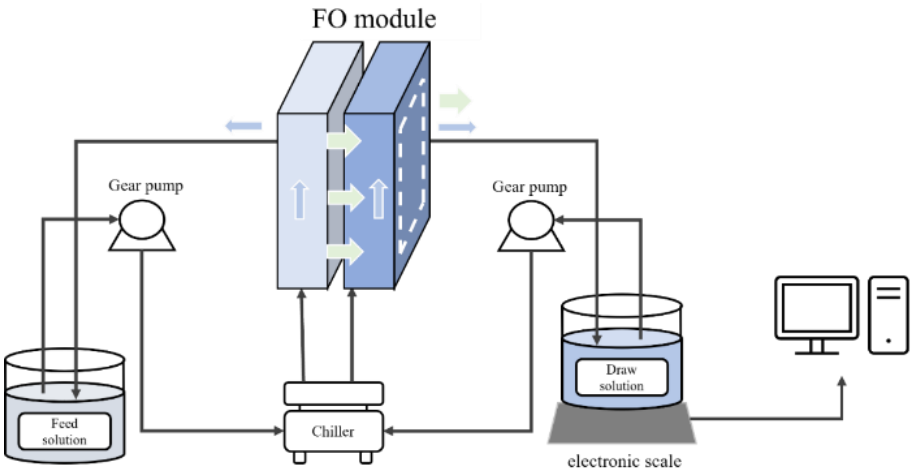

Fig. 2 Schematic diagram of a lab-scale FO experimental set-up

2.2 Feed and draw solutions

In this study, synthetic municipal wastewater was employed as the feed solution (FS), and its composition, with a chemical oxygen demand (COD) of 390 mg/L, is outlined in Table 2 (Chekli *et al*. 2017). We used Na_2CO_3, $NaHCO_3$, and NaCl as DSs. Detailed information about these three DSs can be found in Table 3. Osmotic pressure, diffusivity, and viscosity measurements for these three solutes were obtained using OLI Stream Analyzer 3.2 (OLI System Inc., Morris Plains, NJ, USA). All chemicals used in this study were of reagent grade and were procured from Sigma Aldrich (USA).

Table 3 Detail information of draw solutions (1 M) used in this study. Thermodynamic properties were determined at temperature of 20 ºC and 1 M concentration by using OLI Stream Analyzer 3.2

Chemicals	Sodium carbonate	Sodium bicarbonate	Sodium chloride
Formula	Na_2CO_3	$NaHCO_3$	NaCl
Molecular weight (g/mol)	106	84	58.4
Osmotic pressure (atm)	55.93	42.08	46.35
Diffusivity ($\times$ $\mathbf{10^{-9}}$ m^2/s)	0.85	1.17	1.4

2.3 Lab-scale FO experiments

The FO process performance was evaluated in a closed-loop bench-scale FO system as shown in Fig. 2 (Kim *et al*. 2021). This lab-scale FO unit has an effective membrane area of 20.02 cm^2 with a channel dimension of 77 mm long, 26 mm wide, and 3 mm deep. The FO cell had two symmetric channels on both sides of the membrane for co-current flows of FS and DS. Variable speed gear pumps (Cole-Parmer, USA) were used to pump the liquid in a closed loop. The DS tank was placed on a digital scale and the weight changes were measured by a computer in real time to determine water flux. Conductivity and pH meters (HaCH, Germany) were connected to a computer to monitor the reverse salt flux (RSF) of draw solutes in the FS tank.

FO experiments were conducted in either the AL-FS mode (i.e., the active layer is facing the FS) or the AL-DS mode (i.e., the active layer is facing the DS). Before each performance experiment, the FO membrane was stabilized for 30 minutes with DI water as FS and CO_2 adsorbent solution as DS. Once stabilized, the water flux was measured continuously throughout the experiment with a 3 minutes time interval. All experiments were conducted at a crossflow velocity of 8.5 cm/s, and a constant temperature of 25 ºC. The performance of each chemical as DS was assessed with synthetic wastewater simulating municipal wastewater as FS. In all experiments, a concentration of 1 M was used for each DS. The experiments, using synthetic wastewater as FS, were carried out for one day (i.e., 24 hours) during which the water flux was measured continuously (i.e. one measurement every three minutes).

2.4 Membrane characterization

Membrane surface characterization was conducted by collecting membrane coupons after experiments, soaking them in DI water for a few seconds to remove FS and DS, and then dried in a desiccator for 1 day. The surface morphologies of the FO membrane were observed and analysed by scanning electron microscopy (SEM, VEGA3, Tescan, Czech) and energy dispersive X-ray spectroscopy (EDX, X-ACT 10, Oxford, England) following the procedures described in a previous study (Woo *et al*. 2016). Samples taken from each membrane were first lightly coated with Au/Pd and then the SEM imaging was carried out at an accelerating voltage of 10 kV.

2.5 Economic feasibility evaluation

This study employed the cost estimation model proposed by other studies (Park *et al*. 2020, Saleh *et al*. 2020). The draw solute make-up cost was neglected in this study because they are generated in the hybrid system, and the impact of the draw solute make-up cost can be neglected. Specific water production cost is calculated by summation of annual operating costs and annualized capital costs.

2.5.1 Capital cost

- Wastewater intake and pretreatment

$$CC_{WWIP}[\$] = 1.143 \times 996(F_{feed})^{0.8} \quad (3)$$

where, F_{feed} is the feed flow rate fed into the FO process (m^3/d). The ratio of wastewater pretreatment cost compared to the conventional seawater reverse osmosis (SWRO) was assumed to be 1.143 (Vinardell *et al*. 2022).

- FO membrane

$$CC_{memb,FO}[\$] = 30 \times A_{memb,FO} \quad (4)$$

$$A_{memb,FO} = F_{feed} \times R/J_w \quad (5)$$

where, $A_{memb,FO}$ is the FO membrane area (m^2). The FO membrane cost is assumed as 30 $\$/m^2$ (Zhang *et al*. 2011).

- Draw solute

$$CC_{Draw}[\$] = D_{draw} \times C_{D,FO,in} \times F_{D,FO,in} \times 3600 \quad (6)$$

where, D_{draw} is the draw solute cost ($\$/kg$), $C_{D,FO,in}$ is the inlet concentration of the DS in the FO process (kg/m^3), and $F_{D,FO,in}$ is the inlet flow rate of the DS in the FO process (m^3/s).

- Storage Tank

$$1{,}300 < V < 21{,}000\ gal$$

$$CC_{Tank}[\$] = 1.5 \times 1.218 \times f_m \times \exp[2.631 + 1.3673(\ln V) - 0.06309(\ln V)^2 \quad (7)$$

$$21{,}000 < V < 11{,}000\ gal$$

$$CC_{Tank}[\$] = 1.5 \times 1.218 \times f_m \times \exp[11.662 - 0.0614(\ln V) + 0.04536(\ln V)^2 \quad (8)$$

where, f_m was fixed as 2.7 for expressing stainless steel 316 as a material of construction. To calculate the volume of the DS storage tank, the residence time of DS is assumed as 30 minutes.

- High-pressure pump

$$CC_{pump}[\$] = 52F_{HP}\Delta P_{HP} \quad if \ \ F_{HP} < 200m^3/h \quad (9)$$

$$CC_{pump}[\$] = 81(F_{HP}\Delta P_{HP})^{0.96} \quad if \ \ 200m^3/h < F_{HP} < 450m^3/h \quad (10)$$

$$\Delta P_{HP} = \Delta P_{net} + \Delta P_{fc} \quad (11)$$

$$\Delta P_{fc} = 0.01n\bar{q}_{fc}{}^{1.7} \quad (12)$$

where, ΔP_{HP} is the applied pressure (bar), and F_{HP} is the flow rate in the high-pressure pump (m^3/d). This cost function was applied to the DS circulating pump, the FS circulating pump.

$$TCC = 1.411 \times (CC_{SWIP} + CC_{memb,FO} + CC_{Draw} + CC_{Tank} + CC_{pump}) \quad (13)$$

Total annualized capital cost ($TACC$) is calculated by amortization factor.

$$a = \frac{i(i+1)^n}{(i+1)^n - 1} \quad (14)$$

$$TACC = a \times TCC \quad (15)$$

2.5.2 Operating cost

- Electricity

$$OC_{elec}[\$/y] = [W_{dpump} + W_{fpump}] \times D_{energy} \times 365 \times L_f \quad (16)$$

$$W_{dpump} = \Delta P_d \times Q_d \quad (17)$$

$$W_{fpump} = \Delta P_f \times Q_f \quad (18)$$

where, W_{dpump} and W_{fpump} are the energy consumptions (kWh/d) of the DS circulating pump, FS circulating pump, respectively, D_{energy} is the electricity cost ($\$/kWh$), L_f is the load factor, ΔP_d and ΔP_f are the applied pressure of the DS circulating pump, FS circulating pump, and Q_d and Q_f are the flow rate of DS and FS.

- Membrane replacement

$$OC_{memb}[\$/y] = 0.1 \times CC_{memb} \quad (19)$$

- Chemical supply

$$OC_{ch}[\$/y] = 0.0225 \times F_{feed} \times 365 \times L_f \quad (20)$$

- Insurance

$$OC_{insure}[\$/y] = 0.005 \times TCC \quad (21)$$

- Labor and maintenance

$$OC_{labor}[\$/y] = 0.02 \times F_p \times 365 \times L_f \quad (22)$$

$$TAC = TACC + (OC_{elec} + OC_{insure} + OC_{labor}) \quad (23)$$

Total annualized cost (TAC) and specific water cost (SWC) can be calculated as follows.

$$SWC = \frac{TAC}{F_p \times L_f \times 365} \quad (24)$$

3. Results and discussion

3.1 Basic performance of the FO process

3.1.1 Effect of DS type on thermodynamic properties

This study employed three different DSs: Na_2CO_3, $NaHCO_3$, and NaCl. Na_2CO_3 and $NaHCO_3$ were selected as by-products of carbon absorption by NaOH, while NaCl served as a reference. To assess the basic performance of the FO process, the thermodynamic properties, specifically

Table 4 pH change after 2 hr operation

Draw solutions	AL-FS mode				AL-DS mode			
	0.1 M	0.3 M	0.6 M	1 M	0.1 M	0.3 M	0.6 M	1 M
Na_2CO_3	9.8 ± 0.1	10.1 ± 0.1	10.2 ± 0.3	10.4 ± 0.4	9.9 ± 0.1	10.0 ± 0.1	10.4 ± 0.1	10.4 ± 0.1
$NaHCO_3$	7.5 ± 0.6	7.5 ± 1	7.4 ± 0.8	8.2 ± 0.7	7.4 ± 0.1	7.6 ± 0.4	7.5 ± 0.3	7.7 ± 0.1
NaCl	6.2 ± 0.1	6.4 ± 0.1	7.2 ± 1.1	6.9 ± 0.9	6.1 ± 0.1	6.2 ± 0.1	6.2 ± 0.2	6.6 ± 0.6

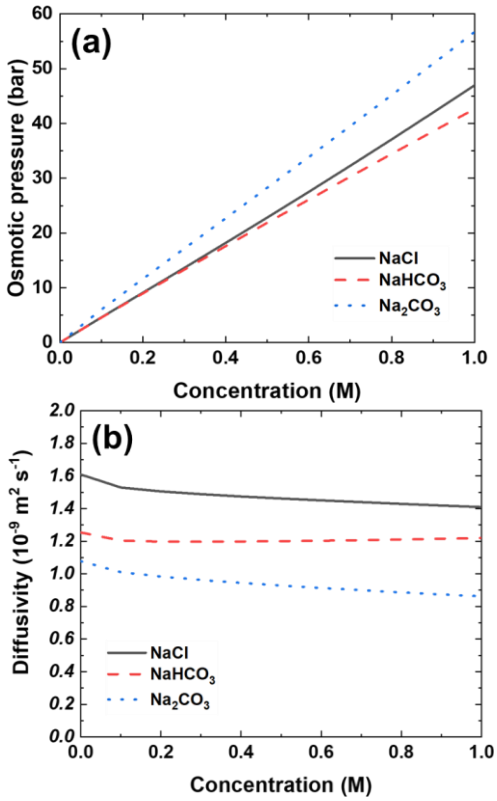

Fig. 3 Changes of osmotic pressure and diffusivity of three DSs (NaCl, $NaHCO_3$ and Na_2CO_3) with increasing their concentrations

osmotic pressure and diffusivity, of the three DSs were examined (see Fig. 3). The osmotic pressure of NaCl, $NaHCO_3$, and Na_2CO_3 increases with concentration due to the higher number of dissolved ions influencing the solution's colligative properties. At equal molar concentrations, Na_2CO_3 exerts the highest osmotic pressure, followed by NaCl and $NaHCO_3$. The concentration of these salts also affects solute diffusivity in the DS, with higher concentrations generally decreasing diffusivity due to increased ionic interactions and viscosity. NaCl, dissociating into two ions, moderately reduces diffusivity. $NaHCO_3$, also dissociating into two ions, similarly reduces diffusivity but may introduce buffering effects that slightly alter the ionic environment. Na_2CO_3, producing three ions per molecule, significantly reduces diffusivity due to the highest increase in ionic interactions and solution viscosity.

3.1.2 FO performance (water flux and RSF) under AL-FS mode

Fig. 4 illustrates the effect of DS concentration on water flux and RSF in the FO process under the AL-FS mode. Increasing the concentration of Na_2CO_3, $NaHCO_3$, and NaCl in the DS enhanced water flux due to the rise in osmotic pressure, with NaCl exhibiting the highest water flux. Water flux in the FO process is determined by osmotic pressure and diffusivity, as shown in Fig. 3. Higher osmotic pressure increases the driving force, while higher diffusivity can intensify internal concentration polarization (ICP), reducing the effective osmotic pressure gradient. Although Na_2CO_3 has very high osmotic pressure, its relatively low diffusivity results in significant ICP, making the increase in water flux for NaCl more pronounced. Na_2CO_3 showed high water flux at low concentrations, but as its concentration increased, its flux trend resembled that of $NaHCO_3$. This is because $NaHCO_3$ maintains consistent diffusivity, whereas Na_2CO_3's diffusivity decreases, leading to greater ICP. $NaHCO_3$ exhibited the lowest osmotic pressure and thus the lowest water flux at low concentrations. However, as concentration increased, $NaHCO_3$'s consistent diffusivity caused its water flux to become similar to that of Na_2CO_3.

The RSF varied depending on the DS type and was influenced by increasing concentrations of Na_2CO_3, $NaHCO_3$, and NaCl. In general, higher concentrations led to greater RSF due to the increased concentration gradient across the membrane. Despite having the highest osmotic pressure and ionic strength, Na_2CO_3, which dissociates into three ions (two Na^+ and one CO_3^{2-}) per molecule, exhibited moderate RSF. This was attributed to the larger size of CO_3^{2-} ions, which made diffusion through the FO membrane more difficult. NaCl, dissociating into two ions per molecule, exhibited the highest RSF due to its superior diffusivity. Conversely, $NaHCO_3$, which also dissociates into two ions but with slightly different ionic properties, displayed similar osmotic pressure but lower diffusivity than NaCl, resulting in the lowest RSF. At higher concentrations, increased viscosity could reduce ion mobility, potentially mitigating RSF to some extent; however, the concentration gradient remained the primary driving force (Zhao and Zou 2011).

The pH levels of the FS varied significantly depending on the type of draw solute used, influencing both water flux and RSF as shown in Table 4. When Na_2CO_3 was used, the FS pH increased to 10.4 due to its strong alkalinity, which likely contributed to higher RSF by enhancing the dissociation and mobility of ions, particularly Na^+. This elevated pH might also have affected the membrane surface charge, potentially increasing the electrostatic interactions that drive cation migration (Kim *et al*. 2017). In contrast, $NaHCO_3$ raised the pH to a more moderate level of 8.2, resulting in lower RSF and reduced electrostatic interactions compared to Na_2CO_3. NaCl, with a FS pH of 7.2, maintained

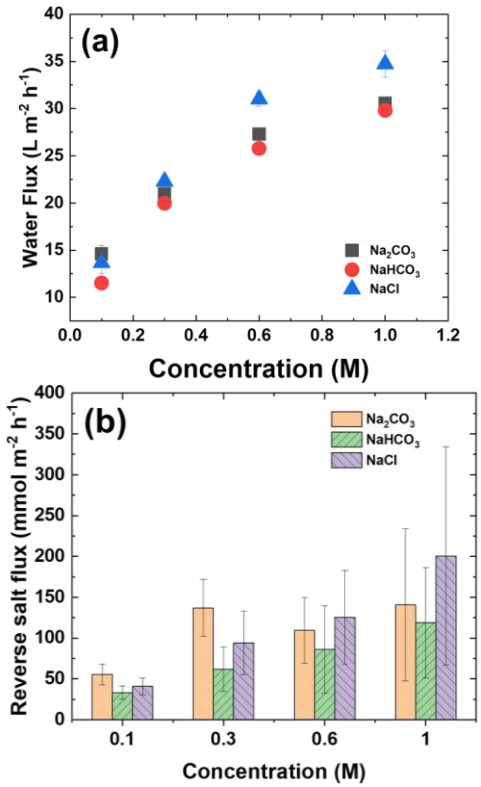

Fig. 4 Water flux and RSF with increasing the concentration of three DSs (NaCl, $NaHCO_3$ and Na_2CO_3) under AL-FS mode

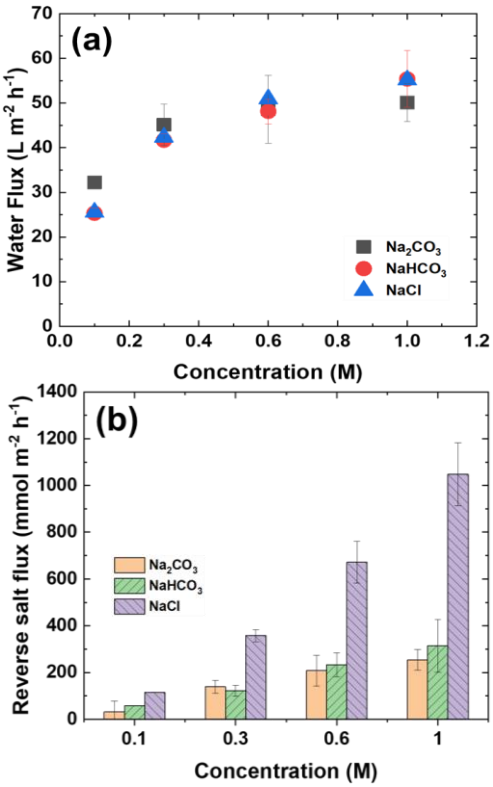

Fig. 5 Water flux and RSF with increasing the concentration of three DSs (NaCl, $NaHCO_3$ and Na_2CO_3) under AL-DS mode

a nearly neutral environment, minimizing electrostatic effects and exhibiting the most stable RSF behavior. These pH differences highlight their role in FO, where the higher alkalinity associated with Na_2CO_3 may exacerbate ICP and ion back-diffusion. Meanwhile, the near-neutral pH of NaCl likely minimizes such effects, enabling a more efficient osmotic gradient utilization. The interplay between pH and membrane performance suggests that DS choice is critical not only for optimizing osmotic pressure but also for managing pH-induced effects on flux and membrane stability.

3.1.3 FO performance (water flux and RSF) under AL-DS mode

When the membrane orientation was switched to the AL-DS mode, distinct trends were observed in water flux depending on the draw solute and its concentration (see Fig. 5). At low concentrations, Na_2CO_3 exhibited the highest water flux due to its high osmotic pressure. However, as the concentration increased, the difference in water flux among Na_2CO_3, $NaHCO_3$, and NaCl became less pronounced. All draw solutions showed an overall increase in water flux with rising concentration, but the extent of the increase was more gradual for Na_2CO_3 and $NaHCO_3$ compared to NaCl. This suggests that external concentration polarization (ECP) and diffusivity effects play a more significant role in the AL-DS mode.

For RSF, Na_2CO_3 and $NaHCO_3$ demonstrated nearly identical values across the tested concentrations, reflecting their similar dissociation patterns and ionic behavior. In contrast, NaCl exhibited a markedly higher RSF, which increased significantly with concentration. This could be attributed to NaCl's relatively higher ion diffusivity and its tendency to generate a steeper concentration gradient in the AL-DS mode. Across all DSs, the RSF consistently rose with increasing concentration, highlighting the impact of higher DS concentrations on the driving force for salt diffusion back into the feed solution.

The FS pH also shifted depending on the DS used, further influencing both water flux and RSF. Na_2CO_3 increased the FS pH to 10.4 due to its strong alkalinity, while $NaHCO_3$ resulted in a more moderate pH of 7.7. NaCl maintained a slightly acidic pH of 6.6 in the feed solution. These pH differences likely affected membrane performance by altering surface charge and electrostatic interactions, which may explain some of the variations in water flux and RSF observed between the solutes (Kimani *et al.* 2022). Overall, the AL-DS mode highlighted the critical interplay between solute properties, concentration, and pH in governing the FO performance.

3.2 Domestic wastewater treatment by the FO process

The FO process holds significant potential for treating domestic wastewater due to its ability to achieve water recovery with minimal energy consumption. In this study, three DSs (NaCl, $NaHCO_3$, and Na_2CO_3) were evaluated under two operational modes, AL-FS and AL-DS, to determine their effectiveness in treating synthetic domestic wastewater as presented in Fig. 6.

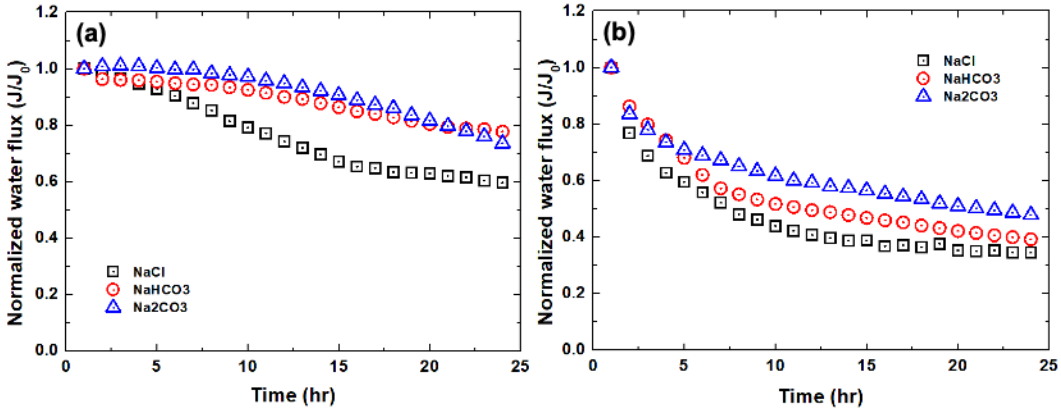

Fig. 6 Changes of normalized water flux under (a) AL-FS mode and (b) AL-DS mode

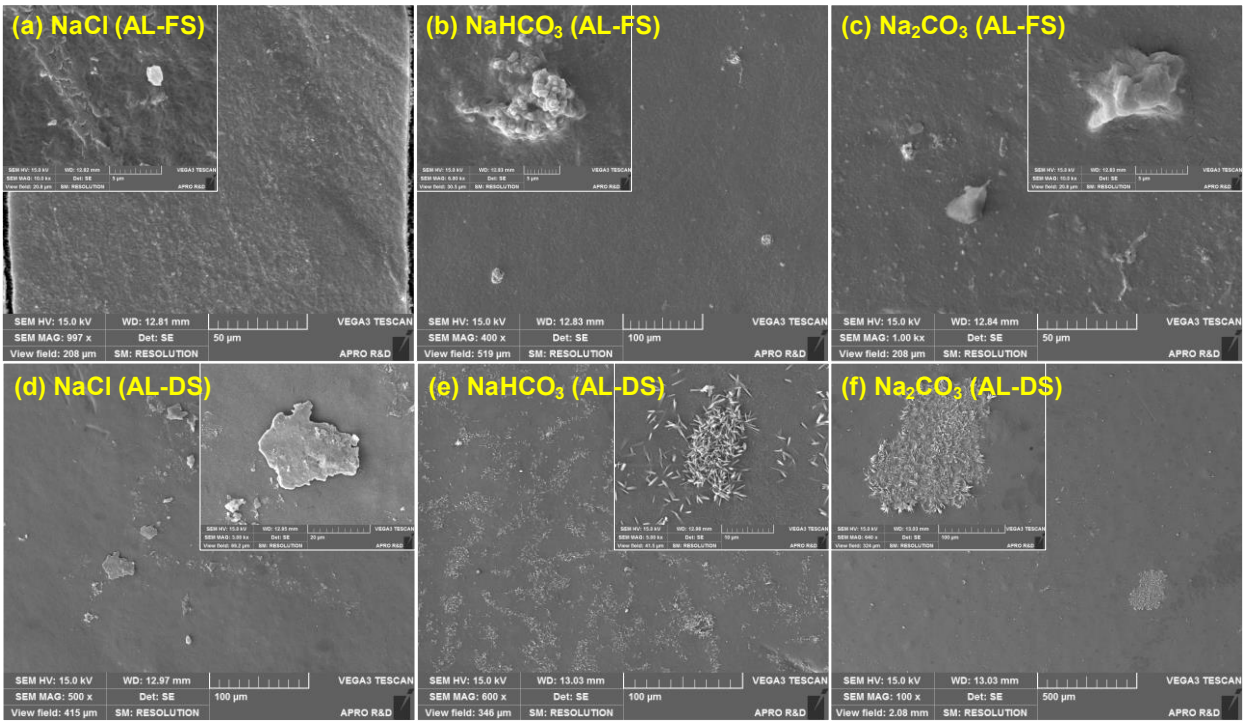

Fig. 7 SEM images of the active layer of fouled FO membrane (AL-FS mode) with (a) NaCl 1 M, (b) $NaHCO_3$ 1 M and (c) Na_2CO_3 1 M and the support layer of fouled FO membrane (AL-DS mode) with (d) NaCl 1 M, (e) $NaHCO_3$ 1 M and Na_2CO_3 1 M

Under the AL-FS mode, the initial water flux (i.e., 17.8 L/m^2/h, 15.2 L/m^2/h and 13.1 L/m^2/h for NaCl, Na_2CO_3 and $NaHCO_3$, respectively) was influenced significantly by the type of DS used. NaCl exhibited the highest initial flux due to its strong osmotic pressure; however, it also experienced the most severe flux decline over time. The rapid flux reduction was attributed to two primary factors: membrane fouling and increased feed solution conductivity caused by RSF. SEM and EDX analyses of the fouled membrane revealed evidence of organic fouling, particularly with NaCl, further corroborating this observation.

In comparison, $NaHCO_3$ and Na_2CO_3 demonstrated similar levels of flux decline, albeit less severe than NaCl. Despite a higher increase in FS conductivity with Na_2CO_3, the flux decline was mitigated due to its ability to elevate the FS pH. The alkaline environment reduced the adhesion of organic foulants, thereby lowering the extent of membrane fouling. SEM images in Fig. 7 (panels a-c) illustrate the differences in fouling patterns across the active layer of membranes. The membrane operated with Na_2CO_3 exhibited the least fouling, characterized by a smoother surface with fewer organic deposits. EDX results (Table 5) further confirm this, showing a higher carbon content on membranes fouled with NaCl and $NaHCO_3$, indicating greater organic contamination compared to Na_2CO_3.

In the AL-DS mode, the performance trends were consistent with those observed in the AL-FS mode, but with lower overall water flux due to enhanced ECP on the DS side. NaCl again exhibited the highest initial flux but suffered from the most significant flux decline over time. Na_2CO_3, on the other hand, maintained relatively stable performance, showing the lowest flux decline among the

Table 5 EDX results (weight%) of fouled membranes

Elements	AL-FS mode			AL-DS mode		
	Na_2CO_3	$NaHCO_3$	NaCl	Na_2CO_3	$NaHCO_3$	NaCl
C	37.1	47.5	57.8	58.7	45.1	65.6
O	41.3	47.4	36.7	22.4	45.0	27.6
Na	13.6	-	4.9	7.9	2.2	2.8
Ca	-	-	-	-	4.8	-
S	8.0	5.1	0.6	1.9	2.9	4.0
Cl	-	-	-	9.1	-	-

Table 6 pH and conductivity of FSs after 24hr operation

Components	AL-FS mode			AL-DS mode		
	Na_2CO_3	$NaHCO_3$	NaCl	Na_2CO_3	$NaHCO_3$	NaCl
pH	11.0 ± 0.6	9.0 ± 0.5	8.4 ± 0.4	11.2	9.9 ± 0.2	8.7 ± 0.2
Conductivity (μS/cm)	2,763 ± 841	1,789 ± 762	3,917 ± 2,195	2,740 ± 255	3,510 ± 1,457	6,735 ± 1,124

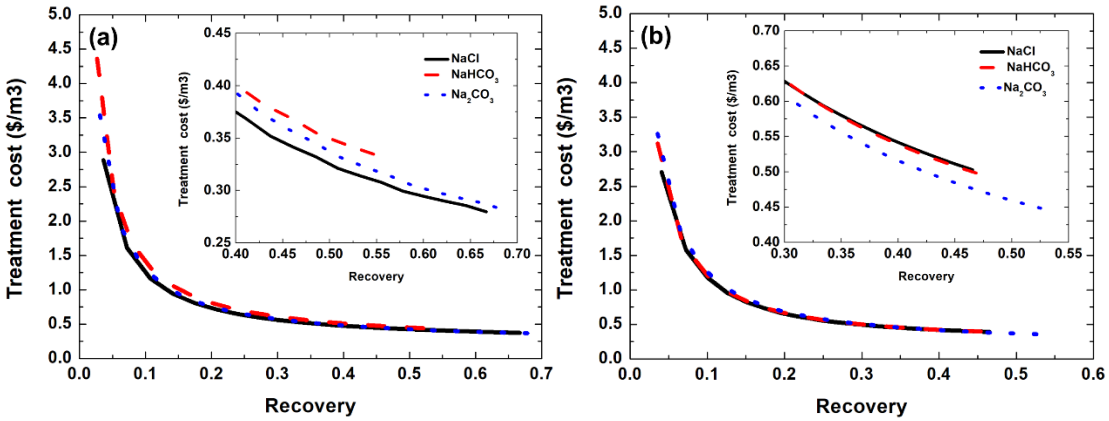

Fig. 8 Treatment costs using FO under (a) AL-FS mode and (b) AL-DS mode

three DSs. This was again attributed to the pH increase in the FS, which mitigated organic fouling and altered the surface charge of the membrane to enhance water transport.

SEM images in Fig. 7 (panels d-f) provide insight into the fouling of the support layer in AL-DS mode. The support layer fouled with Na_2CO_3 exhibited fewer deposits compared to NaCl and $NaHCO_3$, further supporting the fouling mitigation effect of increased pH. EDX data (Table 5) corroborates this observation, with lower carbon and sulfur contents for FO membranes with Na_2CO_3, indicative of reduced organic and inorganic fouling. $NaHCO_3$, while better than NaCl in fouling resistance, showed intermediate fouling levels on both the active and support layers.

Table 6 presents the changes in pH and conductivity of the FS after 24 hours of operation. Na_2CO_3 induced the most substantial pH increase, reaching values above 11, which contributed to fouling mitigation and improved water flux. Despite the high conductivity increase observed with Na_2CO_3, its superior fouling resistance ensured stable flux performance. $NaHCO_3$ showed moderate pH and conductivity changes, while NaCl maintained near-neutral pH, which was insufficient to prevent fouling. These observations highlight the critical interplay between pH control and fouling mitigation in FO processes.

The results suggest that Na_2CO_3 is the most effective DS for treating domestic wastewater in FO systems, offering the lowest fouling resistance and stable flux performance, particularly under alkaline conditions. SEM images (Fig. 7) and EDX results (Table 5) clearly demonstrate reduced organic fouling with Na_2CO_3, further solidifying its suitability for long-term operation. While NaCl provides high initial flux, its susceptibility to fouling and RSF-induced conductivity increases limits of its long-term applicability. $NaHCO_3$ offers a balance between performance and fouling resistance, making it suitable for moderate wastewater treatment scenarios. Operational mode also plays a pivotal role, with AL-FS delivering higher flux and AL-DS offering reduced fouling on the feed side. These insights contribute to the optimization of FO processes for domestic wastewater treatment.

3.3 Economic feasibility

The economic feasibility of the FO process was evaluated by analyzing the treatment costs ($/m³) in relation to recovery levels for three different solutes: NaCl, $NaHCO_3$, and Na_2CO_3. The results reveal a general trend where treatment costs decrease significantly as recovery

increases, particularly at lower recovery levels. This sharp decline highlights the efficiency of the process in reducing costs by recovering more water. However, at higher recovery levels, the reduction in costs plateaus, indicating diminishing returns on cost savings as the recovery approaches its upper limit.

Among the tested DSs in AL-FS mode, NaCl had the lowest treatment cost, with only a minor difference compared to Na_2CO_3. In AL-DS mode, Na_2CO_3 consistently exhibited the lowest treatment costs, highlighting its superior economic performance. Its cost advantage was evident across all recovery levels, making it the most cost-effective solute for FO processes. In contrast, $NaHCO_3$ had the highest treatment costs, making it the least favorable option economically. These cost differences stem from the solutes' chemical properties, which affect their interactions with the membrane and the overall energy demands of the FO process.

The findings suggest that Na_2CO_3 is the optimal choice for achieving both high recovery and low treatment costs, making it particularly suitable for large-scale applications where cost efficiency is critical. While NaCl and $NaHCO_3$ are viable alternatives, their higher costs may limit their use in scenarios where economic constraints are a priority. Furthermore, the observed diminishing returns at higher recovery levels highlight the importance of balancing recovery goals with cost considerations. Operating at an optimal recovery level that maximizes cost efficiency without incurring unnecessary operational expenses can further enhance the economic viability of the FO system.

4. Conclusions

This study demonstrated the potential of integrating CO_2 capture by-products, Na_2CO_3 and $NaHCO_3$, into FO processes for wastewater treatment. Na_2CO_3 emerged as the most effective DS, offering the highest water flux and the lowest fouling rates due to its superior osmotic pressure and alkaline properties. $NaHCO_3$ provided moderate performance, while NaCl, though effective initially, exhibited significant limitations due to high RSF and susceptibility to fouling.

Economic analysis further validated Na_2CO_3 as the most cost-efficient option, with its treatment cost consistently lower than $NaHCO_3$ and NaCl across various recovery levels. The results highlight the feasibility of utilizing Na_2CO_3 in large-scale FO applications, particularly in conjunction with CO_2 capture systems, enabling cost-effective water recovery and sustainable operation. This integrated approach offers a promising solution for addressing global challenges in water scarcity and greenhouse gas emissions, paving the way for innovative applications in wastewater treatment and beyond.

Acknowledgments

This work was supported by the National Research Foundation of Korea (NRF) grant funded by the Korea government (MSIT) (No. 2020R1F1A1068914) and Korea Environment Industry & Technology Institute(KEITI) through R&D Project for Intelligent Optimum Reduction and Management of Industrial Fine Dust, funded by Korea Ministry of Environment(MOE) (2022003580005).

References

Bazarah, A., E.H. Majlan, T. Husaini, A.M. Zainoodin, I. Alshami, J. Goh and M.S. Masdar (2022), "Factors influencing the performance and durability of polymer electrolyte membrane water electrolyzer: A review", *Int. J. Hydrogen Energy*, **47**(85), 35976-35989. https://doi.org/10.1016/j.ijhydene.2022.08.180.

Benyahia, K., M. Khiari and M. Berrabah (2024), "Reuse of reverse osmosis membranes for wastewater treatment (Beni Saf Water Company)", *Membr. Water Treat.*, **15**(4), 153-162. https://doi.org/10.12989/mwt.2024.15.4.153.

Chekli, L., Y. Kim, S. Phuntsho, S. Li, N. Ghaffour, T. Leiknes and H.K. Shon (2017), "Evaluation of fertilizer-drawn forward osmosis for sustainable agriculture and water reuse in arid regions", *J. Environ. Manage.*, **187**, 137-145. https://doi.org/10.1016/j.jenvman.2016.11.021.

Ge, Q., M. Ling and T.S. Chung (2013), "Draw solutions for forward osmosis processes: Developments, challenges, and prospects for the future", *J. Membr. Sci.*, **442**, 225-237. https://doi.org/10.1016/j.memsci.2013.03.046.

Hocking, M.B. (2005), *7 - Industrial Bases by Chemical Routes*. *Handbook of Chemical Technology and Pollution Control (Third Edition)*, 201-220, Academic Press, San Diego, U.S.A.

Hong, W.Y. (2022), "A techno-economic review on carbon capture, utilisation and storage systems for achieving a net-zero CO2 emissions future", *Carbon Capture Sci. Technol.*, **3**, 100044. https://doi.org/10.1016/j.ccst.2022.100044.

Kim, Y., L.H. Kim, J.S. Vrouwenvelder and N. Ghaffour (2021), "Effect of organic micropollutants on biofouling in a forward osmosis process integrating seawater desalination and wastewater reclamation", *J. Hazard. Mater.*, **401**, 123386. https://doi.org/10.1016/j.jhazmat.2020.123386.

Kim, Y., S. Li, L. Chekli, Y.C. Woo, C.H. Wei, S. Phuntsho, N. Ghaffour, T. Leiknes and H.K. Shon (2017), "Assessing the removal of organic micro-pollutants from anaerobic membrane bioreactor effluent by fertilizer-drawn forward osmosis", *J. Membr. Sci.*, **533**, 84-95. https://doi.org/10.1016/j.memsci.2017.03.027.

Kimani, E.M., M. Pranić, S. Porada, A.J.B. Kemperman, I.I. Ryzhkov, W.G.J. van der Meer and P.M. Biesheuvel (2022), "The influence of feedwater pH on membrane charge ionization and ion rejection by reverse osmosis: An experimental and theoretical study", *J. Membr. Sci.*, **660**, 120800. https://doi.org/10.1016/j.memsci.2022.120800.

Li, B., Y. Duan, D. Luebke and B. Morreale (2013), "Advances in CO2 capture technology: A patent review", *Appl. Energy*, **102**, 1439-1447. https://doi.org/10.1016/j.apenergy.2012.09.009.

Majasan, J.O., J.I.S. Cho, I. Dedigama, D. Tsaoulidis, P. Shearing and D.J.L. Brett (2018), "Two-phase flow behaviour and performance of polymer electrolyte membrane electrolysers: Electrochemical and optical characterisation", *Int. J. Hydrogen Energy*, **43**(33), 15659-15672. https://doi.org/10.1016/j.ijhydene.2018.07.003.

Megías-Sayago, C., R. Bingre, L. Huang, G. Lutzweiler, Q. Wang and B. Louis (2019), "CO2 adsorption capacities in zeolites and layered double hydroxide materials", *Front. Chem.*, **7**. https://doi.org/10.3389/fchem.2019.00551.

Paidar, M., V. Fateev and K. Bouzek (2016), "Membrane electrolysis—History, current status and perspective", *Electrochimica Acta* **209**, 737-756. https://doi.org/10.1016/j.electacta.2016.05.209.

Park, K., D.Y. Kim, Y.H. Jang, M.G. Kim, D.R. Yang and S. Hong (2020), "Comprehensive analysis of a hybrid FO/ crystallization/RO process for improving its economic feasibility to seawater desalination", *Water Res.*, **171**, 115426. https://doi.org/10.1016/j.watres.2019.115426.

Said, R.B., J.M. Kolle, K. Essalah, B. Tangour and A. Sayari (2020), "A unified approach to CO2–amine reaction mechanisms", *ACS Omega*, **5**(40), 26125-26133. https://doi.org/10.1021/acsomega.0c03727.

Saleh, J.M., E.M. Ali, J.A. Orfi and A.M. Najib (2020), "Water cost analysis of different membrane distillation process configurations for brackish water desalination", *Membr. Water Treat.*, **11**(5), 363-374. https://doi.org/10.12989/mwt.2020.11.5.363.

Salminen, J.P. and P. Kobylin (2006), "Carbon dioxide-metal carbonate systems in chemical processes and environmental applications", *ECS Transact.*, **1**(18), 27. https://doi.org/10.1149/1.2214632.

Selamet, Ö.F., M.C. Acar, M.D. Mat and Y. Kaplan (2013), "Effects of operating parameters on the performance of a high-pressure proton exchange membrane electrolyzer", *Int. J. Energy Res.*, **37**(5), 457-467. https://doi.org/10.1002/er.2942.

Shaffer, D.L., J.R. Werber, H. Jaramillo, S. Lin and M. Elimelech (2015), "Forward osmosis: Where are we now?" *Desalination*, **356**, 271-284. https://doi.org/10.1016/j.desal.2014.10.031.

Sosa-Fernandez, P.A., S.J. Miedema, H. Bruning, F.A.M. Leermakers, J.W. Post and H.H.M. Rijnaarts (2021), "Effects of feed composition on the fouling on cation-exchange membranes desalinating polymer-flooding produced water", *J. Colloid Interf. Sci.*, **584**, 634-646. https://doi.org/10.1016/j.jcis.2020.10.077.

Sumida, K., D.L. Rogow, J.A. Mason, T.M. McDonald, E.D. Bloch, Z.R. Herm, T.H. Bae and J.R. Long (2012), "Carbon dioxide capture in metal–Organic frameworks", *Chem. Rev.*, **112**(2), 724-781. 10.1021/cr2003272.

Teuku, H., I. Alshami, J. Goh, M.S. Masdar and K.S. Loh (2021), "Review on bipolar plates for low-temperature polymer electrolyte membrane water electrolyzer", *Int. J. Energy Res.*, **45**(15), 20583-20600. https://doi.org/10.1002/er.7182.

Tiraferri, A., N.Y. Yip, A.P. Straub, S. Romero-Vargas Castrillon and M. Elimelech (2013), "A method for the simultaneous determination of transport and structural parameters of forward osmosis membranes", *J. Membr. Sci.*, **444**, 523-538. https://doi.org/10.1016/j.memsci.2013.05.023.

Tiwari, S.C., A. Bhardwaj, K.D.P. Nigam, K.K. Pant and S. Upadhyayula (2022), "A strategy of development and selection of absorbent for efficient CO2 capture: An overview of properties and performance", *Proc. Safe. Environ. Protect.*, **163**, 244-273. https://doi.org/10.1016/j.psep.2022.05.025.

Toan, S., W. O'Dell, C.K. Russell, S. Zhao, Q. Lai, H. Song, Y. Zhao and M. Fan (2019), "Thermodynamics of NaHCO3 decomposition during Na2CO3-based CO2 capture", *J. Environ. Sci.*, **78**, 74-80. https://doi.org/10.1016/j.jes.2018.07.005.

Vinardell, S., G. Blandin, F. Ferrari, G. Lesage, J. Mata-Alvarez, J. Dosta and S. Astals (2022), "Techno-economic analysis of forward osmosis pre-concentration before an anaerobic membrane bioreactor: Impact of draw solute and membrane material", *J. Clean. Prod.*, **356**, 131776. https://doi.org/10.1016/j.jclepro.2022.131776.

Woo, Y.C., Y. Kim, W.G. Shim, L.D. Tijing, M. Yao, L.D. Nghiem, J.S. Choi, S.H. Kim and H.K. Shon (2016), "Graphene/PVDF flat-sheet membrane for the treatment of RO brine from coal seam gas produced water by air gap membrane distillation", *J. Membr. Sci.*, **513**, 74-84. http://doi.org/10.1016/j.memsci.2016.04.014.

Yincheng, G., N. Zhenqi and L. Wenyi (2011), "Comparison of removal efficiencies of carbon dioxide between aqueous ammonia and NaOH solution in a fine spray column", *Energy Procedia*, **4**, 512-518. https://doi.org/10.1016/j.egypro.2011.01.082.

Yoo, M., S.J. Han and J.H. Wee (2013), "Carbon dioxide capture capacity of sodium hydroxide aqueous solution", *J. Environ. Manage.*, **114**, 512-519. https://doi.org/10.1016/j.jenvman.2012.10.061.

Zhang, F., K.S. Brastad and Z. He (2011), "Integrating forward osmosis into microbial fuel cells for wastewater treatment, water extraction and bioelectricity generation", *Environ. Sci. Tech.*, **45**(15), 6690-6696. 10.1021/es201505t.

Zhao, S. and L. Zou (2011), "Relating solution physicochemical properties to internal concentration polarization in forward osmosis", *J. Membr. Sci.*, **379**(1), 459-467. https://doi.org/10.1016/j.memsci.2011.06.021.

YK